KKU SCIENCE JOURNAL
Journal Home Page : https://ph01.tci-thaijo.org/index.php/KKUSciJ
Published by the Faculty of Science, Khon Kaen University, Thailand

การศึกษาการแทรกตัวของโซเดียมในวัสดุ NMC ที่ผ่านการนำลิเทียมออกจากโครงสร้าง: สู่การประยุกต์ใช้วัสดุรีไซเคิลในแบตเตอรี่ชนิดโซเดียมไอออน

Exploring Sodium Insertions into Delithiated NMC Structures: Toward the Utilization of Recycled Materials in Sodium-Ion Batteries

พงษ์สิทธิ์ กระเบา[1] ทรงยุทธ แก้วมาลา[2] วันวิสา ลิ้มพิรัตน์[3] และ นงลักษณ์ มีทอง[2*]

Phongsit Krabao[1], Songyoot Kaewmala[2], Wanwisa Limphirat[3] and Nonglak Meethong[2*]

[1]สาขาวิชาฟิสิกส์ คณะวิทยาศาสตร์ มหาวิทยาลัยขอนแก่น จังหวัดขอนแก่น 40002

[2]หลักสูตรวิทยาศาสตร์แบตเตอรี่และพลังงานใหม่ คณะวิทยาศาสตร์ มหาวิทยาลัยขอนแก่น จังหวัดขอนแก่น 40002

[3]สถาบันวิจัยแสงซินโครตรอน (องค์การมหาชน) จังหวัดนครราชสีมา 30000

[1]Department of Physics, Faculty of Science, Khon Kaen University, Khon Kaen 40002, Thailand

[2]Battery and New Energy Science Program, Department of Physics, Faculty of Science, Khon Kaen University, Khon Kaen, 40002, Thailand

[3]Synchrotron Light Research Institute, Nakhon Ratchasima, 30000, Thailand

บทคัดย่อ

แบตเตอรี่ชนิดโซเดียมไอออน (Sodium-ion batteries: SIBs) ได้รับความสนใจเพิ่มขึ้นอย่างต่อเนื่องในฐานะทางเลือกที่มีศักยภาพแทนแบตเตอรี่ชนิดลิเทียมไอออน เนื่องจากโซเดียมมีอยู่มากในธรรมชาติและราคาถูก อีกทั้งยังตอบโจทย์ความต้องการระบบกักเก็บพลังงานที่ยั่งยืนและต้นทุนไม่สูง งานวิจัยนี้นำเสนอแนวคิดใหม่ที่สามารถรองรับอนาคตของการจัดการทรัพยากรและพลังงาน โดยแสดงให้เห็นว่าวัสดุ LiNMC สามารถนำมาใช้เป็นวัสดุแคโทดในแบตเตอรี่ชนิดโซเดียมไอออนได้อย่างมีประสิทธิภาพ หลังจากผ่านกระบวนการนำลิเทียมออกและเติมโซเดียมเข้าไปใหม่ด้วยกรรมวิธีทางไฟฟ้าเคมี ส่งผลให้เกิดเป็นวัสดุเฟสใหม่ที่เรียกว่า Na_yNMC วัสดุ Na_yNMC ดังกล่าวถูกนำมาศึกษาสมบัติทางไฟฟ้าเคมี โดยเน้นผลขององค์ประกอบโลหะทรานซิชันที่มีต่อการเคลื่อนที่ของไอออนโซเดียม และความสามารถในการคงโครงสร้างเลเยอร์แบบ O3 ซึ่งเป็นลักษณะเฉพาะของวัสดุประเภทออกไซด์ของโลหะทรานซิชันที่มีโครงสร้างแบบเลเยอร์ และใช้กันอย่างแพร่หลายในแบตเตอรี่ชนิดลิเทียมไอออน โดยพบว่าปริมาณลิเทียมที่หลงเหลืออยู่ในโครงสร้างมีส่วนช่วยเพิ่มเสถียรภาพของโครงสร้างดังกล่าว จากผลการทดลองพบว่า ความจุไฟฟ้า อัตราการจ่ายกระแสไฟฟ้า และความเสถียรในการใช้งานของวัสดุ Na_yNMC มีความแตกต่างกันตามอัตราส่วนของโลหะทรานซิชัน โดยเฉพาะสูตร $Na_yNMC811$ ที่ให้ผลลัพธ์โดยรวมดีที่สุด ทั้งในด้านความจุไฟฟ้าใช้งานจริง อัตราการอัด-คายประจุที่ดี และความคงตัวของโครงสร้างในระยะยาว

*Corresponding Author, E-mail: nonmee@kku.ac.th

Received date: 3 July 2025 | Revised date: 21 September 2025 | Accepted date: 29 September 2025
doi: 10.14456/kkuscij.2025.43

ABSTRACT

As the demand for sustainable and cost-effective energy storage increases, sodium-ion batteries (SIBs) are gaining attention as a viable alternative to lithium-ion systems, owing to sodium's abundance and lower cost. In this work, we present an innovative strategy to bridge these technologies by reutilizing NMC cathodes layered transition metal oxides commonly used in lithium-ion batteries as active materials in SIBs. The LiNMC cathodes were delithiated in Li half-cells and subsequently sodiated in Na half-cells to form sodiated Li_{1-x}NMC phases (Na_yNMC). The electrochemical characteristics of the new sodium phases Na_yNMC were compared, focusing on the effect of transition metal composition on sodium-ion transport and stabilization of the layered structure. Initial charge capacities were closely related to the lithium ions retained in the structure, which stabilized the O3-type layered structure. The capacities, rate capability, and cycling stability of the Na_yNMC materials were influenced by the transition metal composition. Notably, Na_yNMC811 exhibited the best overall performance in terms of usable capacity, rate capability, and cycling stability. These findings reveal how transition metal composition governs structural stability and performance, offering a clear strategy for designing next-generation sodium-ion cathodes from recycled materials.

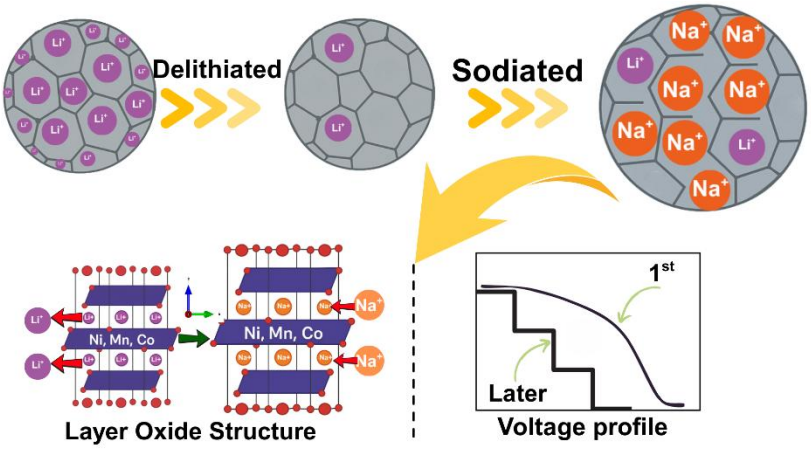

Graphical abstract

Electrochemical sodiation of delithiated NMC cathodes enables their use in sodium-ion batteries. This study compares five NMC compositions (111, 442, 532, 622, 811), demonstrating composition-dependent structure and performance, and emphasizes the need to optimize Na_yNMC stability for next-generation sodium-ion cathodes derived from recycled NMC materials.

คำสำคัญ: แบตเตอรี่ลิเทียมไอออน แบตเตอรี่โซเดียมไอออน ไฟฟ้าเคมี

Keywords: Li-ion Battery, Sodium-ion Battery, Electrochemistry

INTRODUCTION

Due to the natural abundance of sodium and the analogous intercalation processes of Na^+ and Li^+ ions, sodium-ion batteries (SIBs) emerge as a promising alternative to lithium-ion batteries (LIBs) for large-scale energy storage applications (Nayak *et al*., 2018). Nonetheless, developing a SIB cathode that offers high capacity along with robust cycle and thermal stabilities remains challenging, largely because of the larger ionic radius of Na^+ (1.02 Å versus 0.76 Å for Li^+) (Hwang *et al*., 2015). In addition, almost all the Na_xMO_2 (M = transition metal), are not stable against moisture and/or air at ambient conditions (Mu *et al*., 2015). To tackle these issues, numerous sodium-based compounds have been designed and evaluated (Berthelot *et al*., 2010; Han *et al*., 2014; Hasa et al., 2014; Hwang *et al*., 2015; Kim *et al*., 2012; Mu *et al*., 2015; Nose *et al*., 2013; Oh *et al*., 2014; Wang *et al*., 2015; Yabuuchi *et al*., 2013; Yuan *et al*., 2014). In particular, layered transition metal oxides have gained significant interest, inspired by the successful performance of layered $LiMO_2$ cathodes in LIB systems.

Numerous studies have explored to obtain high-energy cathode materials for sodium-ion batteries based on layered oxides containing 3d transition metals (such as Co, Ni, Mn, V, and Fe) (Clément *et al*., 2015; Hwang *et al*., 2017; Yabuuchi *et al*., 2014). For example, $NaCoO_2$ has been recognized as an effective intercalation cathode, delivering an average capacity of approximately 140 mAh·g-¹ via multi-step phase transitions (Berthelot *et al*., 2010). In layered monoxides, the migration of Na^+ ions is complex and involves several phase transitions (e.g., from O-type to P-type structures), which can result in irreversible structural collapse and rapid capacity loss. Consequently, the design of mixed-metal cation oxides aims not only to stabilize the crystal structure but also to enhance electrochemical performance (Kubota and Komaba, 2015; Xiang *et al*., 2015; Yabuuchi *et al*., 2014). The ternary layered oxides such as $NaNi_{1/3}Mn_{1/3}Co_{1/3}O_2$ (NaNMC111), which is the counterpart of $LiNi_{1/3}Mn_{1/3}Co_{1/3}O_2$ (LiNMC111), have been attempted. These cathode materials have been synthesized via a range of methods, including the sol-gel process and coprecipitation. For example, Hwang *et al*. prepared NaNMC compounds by coprecipitating metal salts, followed by calcination at approximately 750ºC for 24 hours, and demonstrated superior performance in sodium half-cells. Their work also clarified the roles of the individual transition metals: increasing the Ni fraction boosts capacity at the expense of capacity retention, Co contributes significantly to structural stabilization, and Mn enhances both capacity retention and thermal stability (Hwang *et al.*, 2016). Sathiya *et al*. (2012) synthesized NaNMC111 via a sol-gel process followed by calcination at 900ºC for 12 hours. The resulting material exhibited a discharge capacity of 120 $mAh \cdot g^{-1}$ and demonstrated very stable cycling performance. However, the material is moisture sensitive and undergoes multi-step phase transitions. Furthermore, the complexity of the composition makes it challenging to obtain a single-phase NaNMC through air sintering (Xu *et al*., 2017). In contrast, LiNMC synthesis is less sensitive to moisture, and a stable O_3 structure with minimal cation disorder can be achieved through a simple calcination process (Hashem *et al*., 2013; Yabuuchi and Ohzuku, 2005). Therefore, almost all conventionally synthesized Na_xMO_2 (M = transition metal) compounds exhibit poor stability against moisture and air at ambient conditions, resulting in performance that is

insufficient for practical applications, particularly for energy storage systems (ESS) that demand long-term stability.

Recently, electrochemical ion-exchange technique has been used to convert high crystallinity lithium-ion oxide cathodes into robust sodium-ion cathode materials. This approach has shown to be an effective strategy to preserve the O3-type layered structure improving structural stability while delivering high capacity and excellent rate performance (Bublil *et al*., 2018; Heubner *et al*., 2020). Tran Van Man *et al*. studied sodiation into $LiNi_{1/3}Mn_{1/3}Co_{1/3}O_2$ (NMC111) showing that the number of Na^+ ion inserted into the delithiated host is comparable to the number of lithium extracted at C/10 rate in the voltage range 2 - 4 V. The diffusion coefficient of Na^+ ion into the solid structure calculated from Galvanostatic Intermittence Titration Technique (GITT) is relatively stable with the value range of 1×10^{-9} - 7×10^{-10} cm^2 s^{-1} that showed an equivalent cation diffusion between Na-migration and Li-migration in the range from 10^{-11} cm^2/s to 10^{-10} cm^2/s (Van Man *et al*., 2018; Nguyen *et al*., 2021).

The ion-exchange process for converting LiNMC to NaNMC remains relatively underexplored, representing a promising strategy for advancing sodium-ion cathode performance. In this work, we began with commercial $Li(N_aMn_bCo_c)O_2$ powders, specifically NMC111, NMC442, NMC532, NMC622, and NMC811 to systematically investigate the role of transition metal composition under controlled conditions. All materials investigated in this study are new rather than end-of-life, which will be considered in future work. This foundational understanding aims to guide future application of the same strategy to recycle NMC from spent lithium-ion batteries. This study is anticipated to yield novel insights and alternative strategies for developing highly stable and efficient cathode materials for sodium-ion batteries.

MATERIALS AND METHODS

1. Electrochemical Characterization

The cathode, $Li(Ni_aMn_bCo_c)O_2$ powders used as starting raw materials are NMC111 ($LiNi_{1/3}Mn_{1/3}Co_{1/3}O_2$), NMC442 ($LiNi_{0.4}Mn_{0.4}Co_{0.2}O_2$), NMC532 ($LiNi_{0.5}Mn_{0.3}Co_{0.2}O_2$), NMC622 ($LiNi_{0.6}Mn_{0.2}Co_{0.2}O_2$), and NMC811 ($LiNi_{0.8}Mn_{0.1}Co_{0.1}O_2$). For further study, the NMC powders were processed into cathode electrodes composed of 80 wt.% NMC, 15 wt.% Super P carbon black, and 5 wt.% polyvinylidene fluoride (PVDF) binder. The mixture was homogenized by ball milling and subsequently coated onto aluminum foil. The coated Al foil was dried at 110ºC in a vacuum oven for 12 hours and punched into round shapes. The electrodes were assembled in Swagelok with glass fiber (Whatman GF/F), 1.3M $LiPF_6$ EC:DMC:EMC (2:7:1) + 2%FEC + 2%PS electrolyte with a Li metal anode in an Ar-filled glove box (O_2 and H_2O levels < 0.1 ppm). The cell was charged at C/10 (1 C defined as the extraction of one Li^+ per formula unit in 1 hour) from the open circuit potential (OCP) to 4.5 V versus Li^+/Li then and kept for at least 3 hours to fully extract lithium-ions. Next, the delithiated electrode ($Li_{1-x}NMC$) was taken out in the glovebox and soaked many times with dimethyl carbonate (DMC) solvent and finally dried at room temperature in Ar atmosphere. The $Li_{1-x}NMC$ electrode was reassembled in a sodium half-cell using sodium metal as the anode, glass fiber (Whatman GF/F) as separator, and 1 M $NaClO_4$ in EC/DEC (1:1 v/v) with 5% FEC as electrolyte. The electrochemical

properties of the sodiated Li_{1-x}NMC phases (Na_yNMC) were evaluated by galvanostatic cycling tests and electrochemical impedance spectroscopy (EIS).

2. Structural and Morphology Characterization

The crystal structure of the samples was analyzed using X-ray diffraction (XRD) with Cu-K_a radiation. The analysis was performed using an Empyrean XRD instrument from PANalytical. The 2θ range for the analysis ranged from 10° to 80°. The morphology and particle size distribution were examined using scanning electron microscopy (SEM) (FEI, Helios NanoLab G3 CX).

RESULTS AND DISCUSSION

Structural characterization using X-ray diffraction (XRD), shown in Figure 1 and Table 1, indicates that all materials crystallize in the O3-layered structure (PDF No. 01-085-1969) belonging to the R3m space group (Zhu *et al*. 2012), and no impurity phases are observed. The lattice parameters obtained from Rietveld refinements with acceptable agreement indices show a slight increase in a (from 2.859 to 2.870 Å) and variation in c (14.206 - 14.252 Å) with higher Ni content, leading to a gradual increase in unit cell volume. This trend reflects the structural adjustment associated with cation substitution across different NMC ratios. According to the SEM images presented in Figure 2 a - e, the commercial NMC materials, including NMC111, NMC442, NMC532, NMC622, and NMC811 display predominantly spherical morphologies. Some regions exhibit both dispersed and aggregated particles, with the average particle size ranging approximately between 10 and 30 µm. The SEM and XRD results collectively suggest similar physical characteristics and crystalline structures among all the samples, with differences attributed solely to the varying chemical compositions and relative proportions of nickel, manganese, and cobalt.

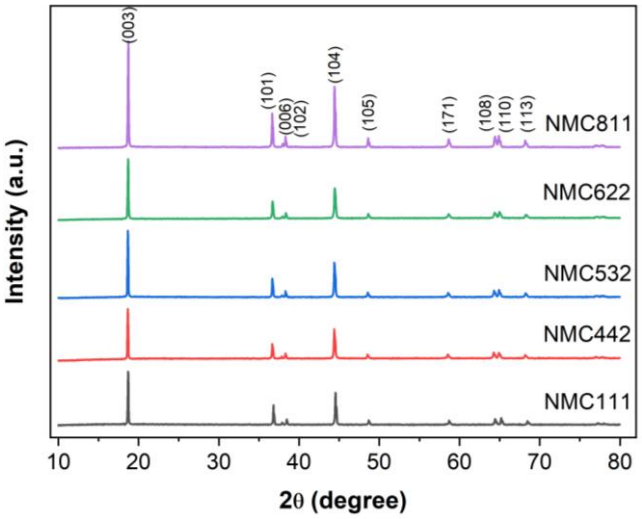

Figure 1 XRD patterns of the cathode powders used in this study including NMC111, NMC442, NMC532, NMC622, and NMC811.

Table 1 Lattice parameters and agreement indices obtained from XRD Rietveld refinements of NMC111, NMC442, NMC532, NMC622, and NMC811 cathode powders.

Sample	Lattice parameters					
	a = b (Å)	c (Å)	v (Å^3)	R_p	R_{wp}	χ^2
NMC111	2.859	14.228	100.747	1.415	1.879	1.141
NMC442	2.869	14.252	101.654	2.169	2.903	2.811
NMC532	2.868	14.239	101.478	1.734	2.298	1.825
NMC622	2.867	14.221	101.238	1.550	2.042	1.326
NMC811	2.870	14.206	101.367	2.189	2.949	2.507

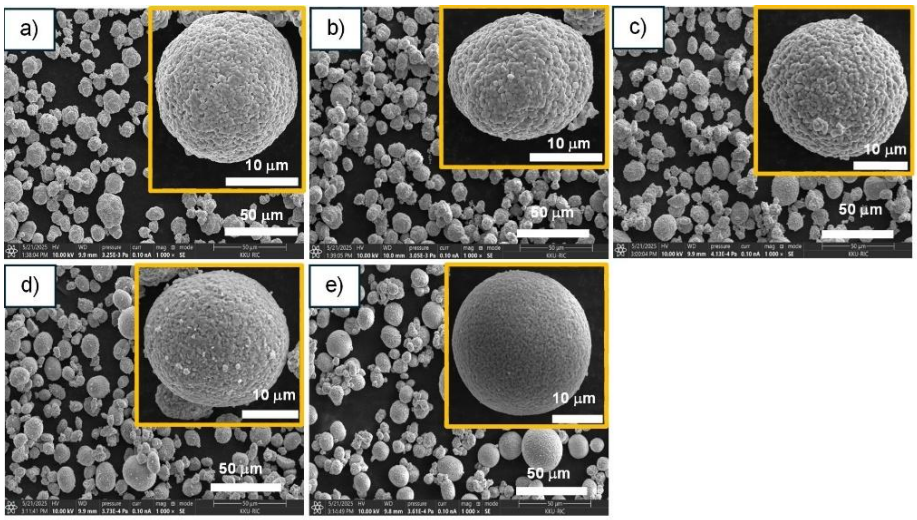

Figure 2 SEM images of cathode powders of a) NMC111, b) NMC442, c) NMC532, d) NMC622, and e) NMC811.

Electrodes based on NMC111, NMC442, NMC532, NMC622, and NMC811 were first delithiated in lithium half-cells using a constant current–constant voltage (CCCV) charging protocol up to 4.5 V to extract the maximum amount of Li^+ ions. Subsequently, these delithiated electrodes were discharged in sodium half-cells to 2 V, forming the corresponding sodiated phases, hereafter denoted as Na_yNMC. For clarity, the sodiated phase derived from $LiNi_{1/3}Mn_{1/3}Co_{1/3}O_2$ (NMC111) is designated as Na_yNMC111, and similar nomenclature applies to the other compositions (Na_yNMC442, Na_yNMC532, Na_yNMC622, and Na_yNMC811). Figure 3 a - b presents the charge/discharge profiles during the delithiation and subsequent sodiation processes showing the amount of Li extracted (delithiation) and Na inserted (sodiation) into the structure. The specific charge capacities achieved at C/10 were approximately 220, 252, 232, 238, and 263 mAh.g^{-1} for Li_{1-x}NMC111, Li_{1-x}NMC442, Li_{1-x}NMC532, Li_{1-x}NMC622, and Li_{1-x}NMC811, respectively, at a cutoff voltage of 4.5 V and a C/10 rate. Dividing the measured capacities by the theoretical capacities yields lithium extractions of about 0.79, 0.91, 0.83, 0.85, and 0.94 mole per formula unit. Upon subsequent discharge in sodium half-cells, the resulting sodiated phases of every transition metal composition exhibit smooth sloping voltage profiles typical of layered oxides intercalating larger Na^+ ions (Van Man *et al*., 2018). Unlike many

conventionally prepared cathodes that show multiple plateaus, these compositions display solid solution type insertion with incremental compositional shifts and no distinct biphasic transitions. The specific discharge capacities achieved at C/10 were approximately 176, 198, 193, 195, 224 mAh.g^{-1} for $Na_yNMC111$, $Na_yNMC442$, $Na_yNMC532$, $Na_yNMC622$, and $Na_yNMC811$, respectively. The Na^+ intercalation was calculated from discharge capacity by assuming one electron per Na^+ and normalizing to the molecular weight of each NMC. The corresponding Na^+ intercalations reach roughly 0.63, 0.71, 0.69, 0.70, and 0.79 mole per formula unit. Nevertheless, the amount of sodium inserted is lower than the lithium extracted during oxidation, reflecting the larger ionic radius of Na^+ and the electrostatic repulsion within the host that prevents complete substitution. In addition, although the discharge curves all show a broadly sloping profile, some compositions exhibit a more pronounced plateau in the lower voltage region around 2.2 and 2.4 V, indicating a localized structural rearrangement (Sathiya *et al*., 2012) or a small biphasic domain during Na^+ insertion. These subtle differences in slope steepness, minor plateaus, and overall shape of the voltage profiles reflect the impact of varying Ni, Mn, and Co content.

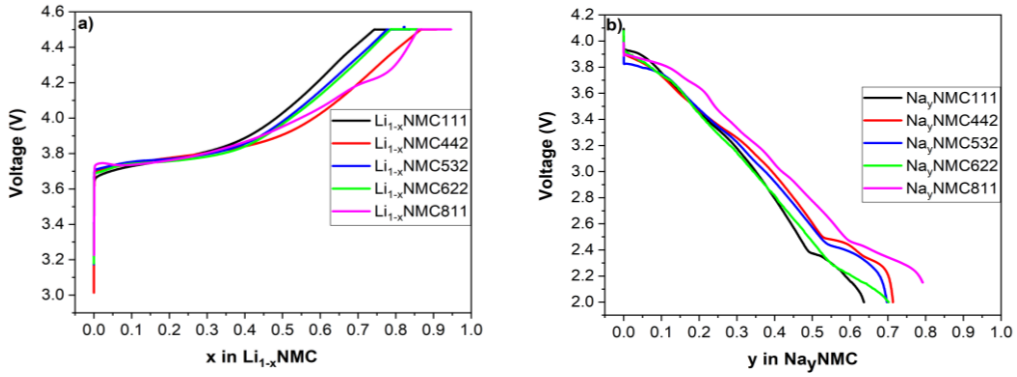

Figure 3 The voltage profiles during a) delithiation (charged), and b) sodiation (discharged), processes for converting LiNMC to NaNMC materials.

Figure 4 a - e presents the voltage profiles associated with sodium intercalation from 1st to 35th cycles across various NMC compositions, highlighting compositional effects on electrochemical behavior. The short plateau observed in the 1st cycle shortened gradually cycle by cycle and disappeared in $Na_yNMC111$ and $Na_yNMC442$ after 20th cycle, but the structural reactions continued in $Na_yNMC532$, $Na_yNMC622$, and $Na_yNMC811$. It could be seen that the shape of the curve did not completely change but the capacity gradually decreased during cycling. The delivered capacity increased proportionally with increasing Ni content. However, as cycling progresses, higher nickel content (as in $Na_yNMC811$) becomes a dominant factor in maintaining capacity and structural integrity. $Na_yNMC811$ is the most promising electrode material due to its superior capacity and stability, followed by $Na_yNMC622$ and $Na_yNMC532$. These results highlight the trade-off between initial stabilization by residual Li^+ and the long-term benefits of high nickel content. Moreover, structural phase changes still occurred upon sodium insertion, as evidenced by the differences in plateau regions during both charge and discharge processes. This indicates that the structure remains unstable, even after only 35 cycles of operation.

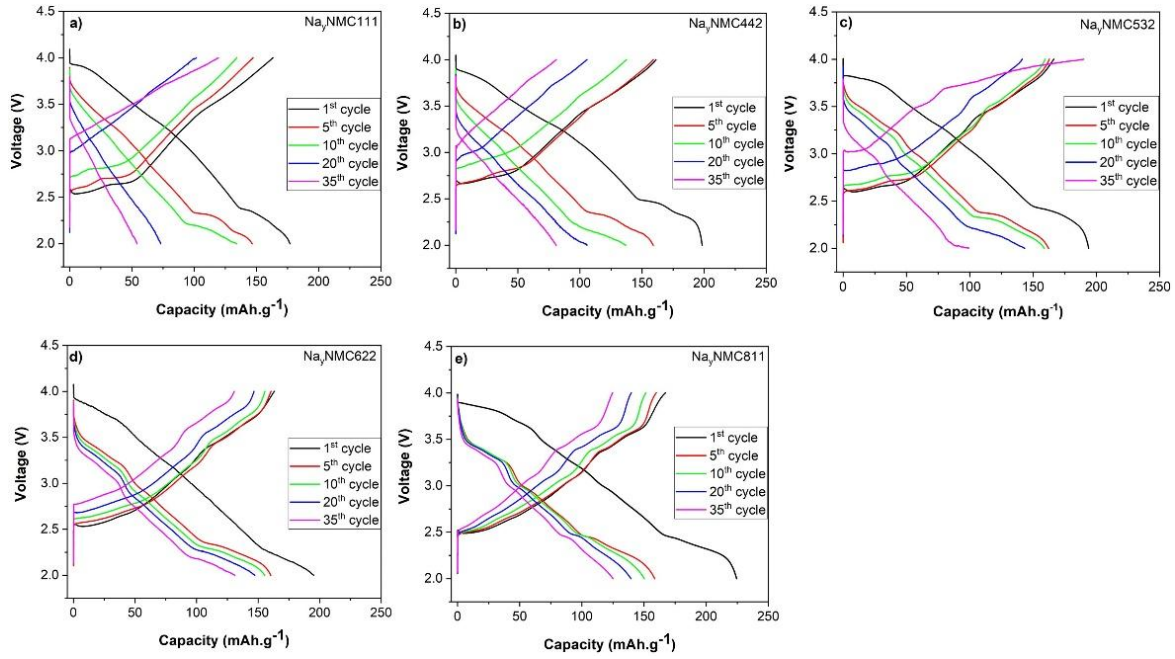

Figure 4 The voltage profiles at 0.1C during cycling from 1st to 35th cycle in Na half-cells for a) $Na_yNMC111$, b) $Na_yNMC442$, c) $Na_yNMC532$, d) $Na_yNMC622$, and e) $Na_yNMC811$.

The rate capability of $Na_yNMC111$, $Na_yNMC442$, $Na_yNMC532$, $Na_yNMC622$, and $Na_yNMC811$ electrodes was performed under 0.1C, 0.2C, 0.5C and 1C rates as shown in Figure 5 a. The capacity of all samples decreased when the rate changed from 0.1C to 1C was applied. The rate capability of $Na_yNMC811$ and $Na_yNMC442$ is relatively better than other samples. $Na_yNMC811$ seems to perform differently from the others, possibly due to its higher nickel content, allowing for greater capacity due to increased active sites for Na^+ storage. In Figure 5 b, the cycling stability at C/10 shows capacity retention after 35th cycle, with the value of 44% for $Na_yNMC111$, 46% for $Na_yNMC442$, 49% for $Na_yNMC532$, 67% for $Na_yNMC622$, and 67% for $Na_yNMC811$, respectively. The results indicate that higher Ni content ($Na_yNMC811$, $Na_yNMC622$) improves structural stability compared to lower-Ni compositions. The balance among Li, Ni, Mn, and Co contents also affects energy density, underscoring the importance of compositional optimization for designing sodium-ion cathodes with both high capacity and long-term stability. This finding highlights a key design principle for achieving long-term stability in sodium-ion batteries. EIS spectra in Figure 5 c - d after sodiation exhibits two semicircles. The first and second semicircles observed at high frequency represent SEI and charge transfer of the electrode, respectively. Regarding the diameter of the first semicircle, the resistance of SEI layered R_{SEI} of $Na_yNMC111$, $Na_yNMC442$, $Na_yNMC532$, $Na_yNMC622$, and $Na_yNMC811$ were 3.967, 0.566, 20.870, 134.9, and 16.94 Ω, respectively. $Na_yNMC442$ demonstrated the smallest resistance from SEI, likely indicating superior electrode-electrolyte interaction and SEI formation. On the other hand, $Na_yNMC622$ shows the highest resistance, suggesting challenges in SEI layer formation or stability. The diameter of the second semicircles showing the charge transfer resistance (R_{ct}) of $Na_yNMC111$, $Na_yNMC442$, $Na_yNMC532$, $Na_yNMC622$, and $Na_yNMC811$ were 3,579, 1,100, 2,563, 2,829, and 1,479 Ω, respectively. $Na_yNMC442$ and $Na_yNMC811$ also exhibited favorable charge transfer resistance, indicating it is the most efficient composition for fast

charge/discharge processes, while $Na_yNMC111$ has the highest R_{ct} indicating poor charge transfer kinetics, which could limit its suitability for high-performance applications. The diffusion coefficients were calculated from the slope of the Z vs $\omega^{-1/2}$ plot as shown in Figure 5 d. The diffusion coefficients of $Na_yNMC111$, $Na_yNMC442$, $Na_yNMC532$, $Na_yNMC622$, and $Na_yNMC811$ were 1.01 x 10^{-10}, 2.39 x 10^{-10}, 2.31 x 10^{-10}, 1.33 x 10^{-10}, and 2.65 x 10^{-10} cm^2 s^{-1} , respectively. These values are in good agreement with previous findings by Van Man *et al.* (Van Man *et al*., 2018). It was found that $Na_yNMC811$ had the highest value of diffusion coefficient, followed by $Na_yNMC442$, $Na_yNMC532$, $Na_yNMC622$, and $Na_yNMC111$ with the lowest value. $Na_yNMC442$ and $Na_yNMC532$ also demonstrated high diffusion coefficients, making them competitive options for efficient sodium-ion transport. The performance of $Na_yNMC811$ electrodes is strongly influenced by nickel content and composition balance. The $Na_yNMC811$ emerges as the most promising candidate for both cycling stability and good ion diffusion due to its high nickel content. Nickel serves as the primary electrochemically active redox center ($Ni^{2+}/Ni^{3+}/Ni^{4+}$), directly governing capacity and operating voltage. In addition, strong Ni–O bonding contributes to structural stabilization, which retards degradation during repeated Na^+ intercalation (Jung *et al.*, 2017a; 2017b; Hwang *et al.*, 2016; Xu *et al.*, 2014). However, excessive Ni can also destabilize the structure if not balanced with Mn and Co, which respectively enhance stability and suppress detrimental phase transitions. The $Na_yNMC442$ also shows exceptional SEI stability, low charge transfer resistance, and competitive diffusion coefficients, making it another viable option. The findings emphasize the critical role of material composition in optimizing electrode performance and the amount of residual lithium in the structure for sodium-ion batteries.

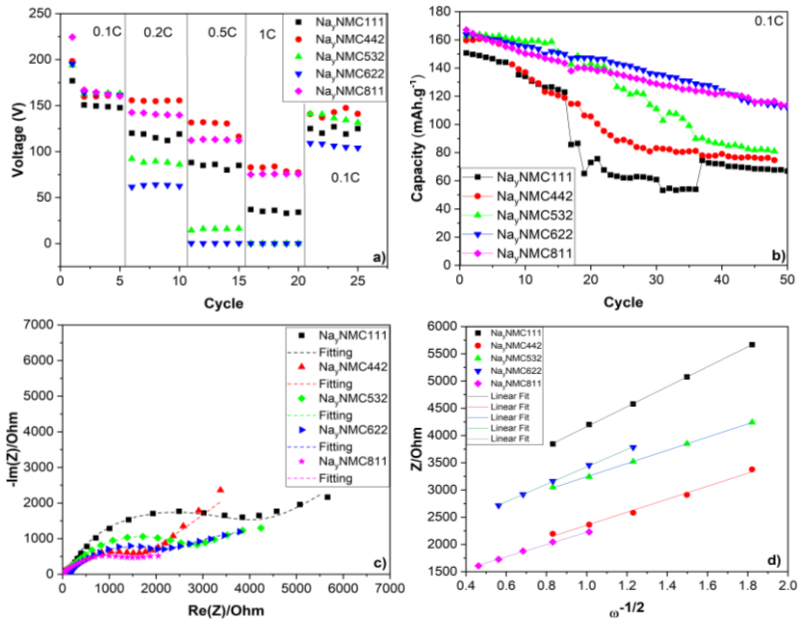

Figure 5 The electrochemical performance showing a) rate performance, b) cycling stability at 0.1C, c) EIS spectra, and d) Z vs $\omega^{-1/2}$ plots of Na_yNMC across various NMC compositions.

CONCLUSIONS

We have successfully prepared sodiated $Li_{1-x}NMC$ phases (Na_yNMC) of various transition metal compositions while preserving their O3-type structure. This work demonstrated that varying the Ni, Mn, and Co content directly impacted the electrochemical performance of Na_yNMC electrodes in sodium-ion batteries. The $Na_yNMC811$, with its high nickel content, showed the best performance, including superior capacity retention, exceptional SEI stability, low charge transfer resistance, and high diffusion coefficients. However, issues such as structural degradation must be resolved to enhance material stability. While this study provides a preliminary demonstration of the impact of Ni content, further research is needed to optimize factors such as residual lithium content, particle size, and transition metal ratios, as well as to validate performance using truly recycled NMC materials. Nevertheless, this work represents an innovative first step toward harnessing green and recovered materials for next-generation sodium-ion batteries.

ACKNOWLEDGEMENT

This research was supported by the Science Achievement Scholarship of Thailand (SAST). It was partially supported by the Institute of Nanomaterials Research and Innovation for Energy (IN-RIE), the Research and Graduate Studies, Khon Kaen University. Furthermore, we acknowledge the insightful discussions and technical guidance from colleagues and collaborators who have contributed to the successful completion of this research. Additional support was provided by the NSRF via the Program Management Unit for Human Resources & Institutional Development, Research and Innovation (No. B42G680031).

REFERENCES

Berthelot, R., Carlier, D. and Delmas, C. (2010). Electrochemical Investigation of the P2–Na_xCoO_2 Phase Diagram. Nature Materials 10(1): 74 - 80. doi: 10.1038/nmat2920.

Bublil, S., Fayena-Greenstein, M., Talyanker, M., Solomatin, N., Tsubery, M.N., Bendikov, T., Penki, T.R., Grinblat, J., Durán, I.B., Grinberg, I., Ein-Eli, Y., Elias, Y., Hartmann, P. and Aurbach, D. (2018). Na-Ion Battery Cathode Materials Prepared by Electrochemical Ion Exchange from Alumina-Coated $Li_{1+x}Mn_{0.54}Co_{0.13}Ni_{0.1+y}O_2$. Journal of Materials Chemistry A 6(30): 14816 - 14827. doi: 10.1039/C8TA05068F.

Clément, R.J., Bruce, P.G. and Grey, C.P. (2015). Review Manganese-Based P2-Type Transition Metal Oxides as Sodium-Ion Battery Cathode Materials. Journal of The Electrochemical Society 162(14): A2589 - A2604. doi: 10.1149/2.0201514jes.

Han, S.C., Bae, E.G., Lim, H. and Pyo, M. (2014). Non-Crystalline Oligopyrene as a Cathode Material with a High-Voltage Plateau for Sodium Ion Batteries. Journal of Power Sources 254: 73 - 79. doi: 10.1016/J.JPOWSOUR.2013.12.104.

Hasa, I., Buchholz, D., Passerini, S., Scrosati, B. and Hassoun, J. (2014). High Performance $Na_{0.5}[Ni_{0.23}Fe_{0.13}Mn_{0.63}]O_2$ Cathode for Sodium-Ion Batteries. Advanced Energy Materials 4(15): 1400083. doi: 10.1002/AENM.201400083.

Hashem, A.M., Abdel-Ghany, A.E., Abuzeid, H.M., Ehrenberg, H., Mauger, A., Groult, H. and Julien, C.M. (2013). $LiNi_{1/3}Mn_{1/3}Co_{1/3}O_2$ Synthesized by Sol-Gel Method: Structure and Electrochemical Properties. ECS Transactions 50(24): 91 - 96. doi: 10.1149/05024.0091ECST.

Heubner, C., Matthey, B., Lein, T., Wolke, F., Liebmann, T., Lämmel, C., Schneider, M., Herrmann, M. and Michaelis, A. (2020). Insights into the Electrochemical Li/Na-Exchange in Layered $LiCoO_2$ Cathode Material. Energy Storage Materials 27: 377 - 386. doi: 10.1016/J.ENSM.2020.02.012.

Hwang, J.Y., Myung, S.T. and Sun, Y.K. (2017). Sodium-Ion Batteries: Present and Future. Chemical Society Reviews 46(12): 3529 - 3614. doi: 10.1039/C6CS00776G.

Hwang, J.Y., Yoon, C.S., Belharouak, I. and Sun, Y.K. (2016). A Comprehensive Study of the Role of Transition Metals in O3-Type Layered $Na[Ni_xCo_yMn_z]O_2$ (x = 1/3, 0.5, 0.6, and 0.8) Cathodes for Sodium-Ion Batteries. Journal of Materials Chemistry A 4(46): 17952 - 17959. doi: 10.1039/C6TA07392A.

Hwang, J.Y., Oh, S.M., Myung, S.T., Chung, K.Y., Belharouak, I. and Sun, Y.K. (2015). Radially Aligned Hierarchical Columnar Structure as a Cathode Material for High Energy Density Sodium-Ion Batteries. Nature Communications doi: 10.1038/ncomms7865.

Jung, R., Metzger, M., Maglia, F., Stinner, C. and Gasteiger, H.A. (2017a). Oxygen Release and Its Effect on the Cycling Stability of $LiNi_xMn_yCo_zO_2$ (NMC) Cathode Materials for Li-Ion Batteries. Journal of The Electrochemical Society 164(7): A1361 - 1377. doi: 10.1149/2.0021707JES/.

Jung, R., Metzger, M., Maglia, F., Stinner, C. and Gasteiger, H.A. (2017b). Chemical versus Electrochemical Electrolyte Oxidation on NMC111, NMC622, NMC811, LNMO, and Conductive Carbon. Journal of Physical Chemistry Letters 8(19): 4820 - 4825. doi: 10.1021/ACS.JPCLETT.7B01927.

Kim, D., Lee, E., Slater, M., Lu, W., Rood, S. and Johnson, C.S. (2012). Layered $Na[Ni_{1/3}Fe_{1/3}Mn_{1/3}]O_2$ Cathodes for Na-Ion Battery Application. Electrochemistry Communications 18(1): 66 - 69. doi: 10.1016/J.ELECOM.2012.02.020.

Kubota, K. and Komaba, S. (2015). Review Practical Issues and Future Perspective for Na-Ion Batteries. Journal of The Electrochemical Society 162(14): A2538 - A2550. doi: 10.1149/2.0151514JES.

Mu, L., Xu, S., Li, Y., Hu, Y.S., Li, H., Chen, L. and Huang, X. (2015). Prototype Sodium-Ion Batteries Using an Air-Stable and Co/Ni-Free O3-Layered Metal Oxide Cathode. Advanced Materials 27(43): 6928 - 6933. doi: 10.1002/ADMA.201502449.

Nayak, P.K., Yang, L., Brehm, W. and Adelhelm, P. (2018). From Lithium-Ion to Sodium-Ion Batteries: Advantages, Challenges, and Surprises. Angewandte Chemie International Edition 57(1): 102 - 120. doi: 10.1002/ANIE.201703772.

Nguyen, V.H., Nguyen, L.M., Huynh, T.T.K., Tran, V.M. and Le, M.L.P. (2021). New Sodium Intercalation Cathode Prepared by Sodiation of Delithiated Host $LiNi_{1/3}Mn_{1/3}Co_{1/3}O_2$. Advances in Materials Science and Engineering 2021: 6280582. doi: 10.1155/2021/6280582.

Nose, M., Nakayama, H., Nobuhara, K., Yamaguchi, H., Nakanishi, S. and Iba, H. (2013). $Na_4Co_3(PO_4)_2P_2O_7$: A Novel Storage Material for Sodium-Ion Batteries. Journal of Power Sources 234: 175 - 179. doi: 10.1016/J.JPOWSOUR.2013.01.162.

Oh, S.M., Myung, S.T., Hwang, J.Y., Scrosati, B., Amine, K. and Sun. Y.K. (2014). High Capacity O3-Type $Na[Li_{0.05}(Ni_{0.25}Fe_{0.25}Mn_{0.5})_{0.95}]O_2$ Cathode for Sodium Ion Batteries. Chemistry of Materials 26(21): 6165 - 6171. doi: 10.1021/CM502481B.

Sathiya, M., Hemalatha, K., Ramesha, K., Tarascon, J.M. and Prakash, A.S. (2012). Synthesis, Structure, and Electrochemical Properties of the Layered Sodium Insertion Cathode Material: $NaNi_{1/3}Mn_{1/3}Co_{1/3}O_2$. Chemistry of Materials 24(10): 1846 - 1853. doi: 10.1021/CM300466B.

Van Man, T., Nguyen, H.L.T., Nam, L.P.P., Linh, N.D., An, P.L.B and Phung, L.M.L. (2018). Electrochemical Na-Migration into Delithiated Phase $Li_zNi_{1/3}Mn_{1/3}Co_{1/3}O_2$: Structure and Electrochemical Properties. Journal of The Electrochemical Society 165(7): A1558. doi: 10.1149/2.1281807jes.

Wang, Y., Xiao, R., Hu, Y.S., Avdeev, M. and Chen, L. (2015). P2-$Na_{0.6}[Cr_{0.6}Ti_{0.4}]O_2$ Cation-Disordered Electrode for High-Rate Symmetric Rechargeable Sodium-Ion Batteries. Nature Communications 2015 6(1): 6954. doi: 10.1038/ncomms7954.

Xiang, X., Zhang, K. and Chen, J. (2015). Recent Advances and Prospects of Cathode Materials for Sodium-Ion Batteries. Advanced Materials 27(36): 5343 - 5364. doi: 10.1002/ADMA.201501527.

Xu, G.L., Amine, R., Xu, Y.F., Liu, J., Gim, J., Ma, T., Ren, Y., Sun, C.J., Liu, Y., Zhang, X., Heald, S.M., Solhy, A., Saadoune, I., Mattis, W.L., Sun, S.G., Chen, Z. and Amine, K. (2017). Insights into the Structural Effects of Layered Cathode Materials for High Voltage Sodium-Ion Batteries. Energy & Environmental Science 10(7): 1677 - 1693. doi: 10.1039/C7EE00827A.

Xu, J., Lee, D.H., Clément, R.J., Yu, X., Leskes, M., Pell, A.J., Pintacuda, G., Yang, X., Grey, C.P. and Meng, Y.S. (2014). Identifying the Critical Role of Li Substitution in P2-$Na_x[Li_yNi_zMn_{1-y-Z}]O_2$ ($0 < x, y, z < 1$) Intercalation Cathode Materials for High-Energy Na-Ion Batteries. Chemistry of Materials 26(2): 1260 - 1269. doi: 10.1021/cm403855t

Yabuuchi, N., Kubota, K., Dahbi, M. and Komaba, S. (2014). Research Development on Sodium-Ion Batteries. Chemical Reviews 114(23): 11636 - 11682. doi: 10.1021/cr500192f

Yabuuchi, N. and Ohzuku, T. (2005). Electrochemical Behaviors of $LiCo_{1/3}Ni_{1/3}Mn_{1/3}O_2$ in Lithium Batteries at Elevated Temperatures. Journal of Power Sources 146(1-2): 636 - 639. doi: 10.1016/J.JPOWSOUR. 2005.03.080.

Yabuuchi, N., Yano, M., Yoshida, H., Kuze, S., and Komaba, S. (2013). Synthesis and Electrode Performance of O3-Type $NaFeO_2$ -$NaNi_{1/2}Mn_{1/2}O_2$ Solid Solution for Rechargeable Sodium Batteries. Journal of The Electrochemical Society 160(5): A3131 - 3137. doi: 10.1149/2.018305JES.

Yuan, D., Hu, X., Qian, J., Pei, F., Wu, F., Mao, R., Ai, Xinping., Yang, H. and Cao, Y. (2014). P2-Type $Na_{0.67}Mn_{0.65}Fe_{0.2}Ni_{0.15}O_2$ Cathode Material with High-Capacity for Sodium-Ion Battery. Electrochimica Acta 116: 300 - 305. doi: 10.1016/J.ELECTACTA.2013.10.211.

Zhu, J., Vo, T., Li, D., Lu, R., Kinsinger, N.M., Xiong, L., Yan, Y. and Kisailus, D. (2012). Crystal Growth of $Li[Ni_{1/3}Co_{1/3}Mn_{1/3}]O_2$ as a Cathode Material for High-Performance Lithium-Ion Batteries. Crystal Growth and Design 12(3): 1118 - 1123. doi: 10.1021/cg200565n.

❑❑❑❑❑